HEAT TRANSFER IN A RECIRCULATION ZONE AT STEADY-STATE AND OSCILLATING CONDITIONS - THE BACK FACING STEP TEST CASE

A.K. Pozarlik[1], D. Panara[2], J.B.W. Kok[1], T.H. van der Meer[1]
[1]Laboratory of Thermal Engineering, University of Twente, Enschede, The Netherlands
[2]Deutsches Zentrum für Luft- und Raumfahrt e.V. (DLR), Stuttgart, Germany

Nomenclature

k	turbulence kinetic energy
ε	turbulent dissipation rate
ω	turbulent frequency
F_2	blending function
μ_t	eddy viscosity
τ_w	wall shear stress
P_k	turbulent production due to viscous and buoyancy forces
Xr	reattachment length

Model constants

k-ε		*k-ω*		*SST*	
C_μ	0.09	β'	0.09	a_1	0.31
$C_{\varepsilon 1}$	1.44	α	5/9		
$C_{\varepsilon 2}$	1.92	β	0.075		
σ_k	1.00	σ_k	2.00		
σ_ε	1.30	σ_ω	2.00		

Abstract

Steady state and transient heat transfer is a very important aspect of any combustion process. To properly simulate gas to wall heat transfer in a turbulent flow, an accurate prediction of the flow and the thermal boundary layer is required. A typical gas turbine combustion chamber flow presents similarities with the academic backward facing step case, especially in the near wall regions where the heat transfer phenomena take place. For this reason, due to its simple geometry and the availability of well documented experiments, the backward facing step with wall heat transfer represents an interesting validation case. Results of steady-state and transient calculations with the use of various turbulence models are compared here with available experimental data.

1 Introduction

The life time of a gas turbine combustor depends critically on the heat transfer between the liner and the hot combusting flow. An important design characteristic of these combustors is the flow of air and fuel entering the combustor at high axial and tangential velocity and small radius and expanding to larger radii. This determines the flame stabilization, and results in a short flame length. A major complication here is that the hot combusting flow is forced outward due to centripetal forces and is directed towards the liner wall. Hence the hot gases flow at high velocity and thin boundary layer past the liner wall, inducing a high rate of heat transfer, heating the liner to temperatures of 800 C or more. The equilibrium liner temperature depends on the balance between heat loss to the cooling air at the cold liner side and heat input at the hot liner side. To complicate the situation, the hot side heat transfer can have a transient and oscillating character due to spontaneous oscillations of the hot flow. These can be caused by coupled flame to burner acousto/aero dynamic feedback processes.
In this paper the transient and oscillatory heat transfer in gas turbine combustor geometry is investigated in more detail and in isolation of other difficult to model processes like combustion,

swirling flow and acoustics. To this end the combustor is reduced to its most elementary geometry, namely a backward facing step. Investigated is the simulation of the gas to wall heat transfer in a turbulent flow over the step, with specific attention to the accurate prediction of the flow, thermal boundary layer and resulting wall friction coefficient and heat transfer coefficient. The flow over the backward facing step with heat transfer is well documented with experimental data. Experimental data used here are by Vogel & Eaton (Vogel & Eaton, 1985).
The characteristic attribute of the flow over the backward facing step is a separation of the boundary layer at the edge of the step. Behind the step, as an effect of an adverse pressure gradient a primary recirculation region is formed. The length of this region is specified by factors related to the flow properties as well as geometrical dimensions of the sudden expansion channel. Typically for the backward facing step the maximum heat transfer coefficient is observed within the recirculation region close to the reattachment point. This position and value of the peak in the heat transfer coefficient is correlated in stationary flows to the position and value of the skin friction coefficient. These phenomena are investigated with URaNS modelling and application of various turbulence models for stationary and oscillatory flows.
To investigate the influence of the flow and geometrical backward facing step parameters on the variations in the heat transfer and wall friction coefficient, several stationary and transient calculations were performed. The stationary solutions obtained using various turbulent models were compared with experimental data. For stationary calculations the standard k-ε, k-ω and shear stress transport (SST) models as available in the Ansys CFX code were used (CFX 10, 2005). The transient calculations were performed with the turbulence model that presented the best agreement with the experimental results in the stationary situation. The influence of a pulsating inlet velocity on the recirculation region and the rate of heat transfer coefficient were explored. The axial inlet velocity was oscillated in the frequency range 10-1,000 Hz.

2 Theory

The conservation equations describing a time-dependent viscous flow are the following:

Continuity:
$$\frac{\partial \rho}{\partial t} + (\nabla \cdot \rho v) = 0 \tag{1}$$

Momentum:
$$\rho \frac{Dv}{Dt} = -\nabla p - [\nabla \cdot \tau] + \rho g \tag{2}$$

Energy:
$$\rho C_p \frac{DT}{Dt} = -(\nabla \cdot \underline{q}) - \frac{Dp}{Dt} - (\tau : \nabla v) \tag{3}$$

The flow shear stress and the energy heat flux are indicated with τ and $\underline{q}$ respectively and can be modelled with the classic Newtonian fluid constitutive equation and the Fourier heat transfer law. The presentation of the results in this paper is done with the use of dimensionless numbers, i.e. Stanton number and skin friction coefficient, which are defined in terms of the heat transfer coefficient and wall shear stress, respectively. The Stanton number describes the ratio of the heat transferred into the fluid to the thermal capacity of the fluid itself. Whereas the skin friction coefficient is a function of the shearing stress exerted by the fluid on the wall surface over which it flows.

Stanton number:
$$St = \frac{h}{C_P \cdot \rho \cdot U} \tag{4}$$

Skin friction coefficient:
$$Cf = \frac{\tau_w}{0.5 \cdot \rho \cdot U^2} \tag{5}$$

As already mentioned, it exists for steady flow a correlation between the Stanton number and the skin friction coefficient which might not hold for unsteady flow. Thus in unsteady flows both factors are of interests.
Providing a numerical resolution up to the smallest turbulent structures, the Navier-Stokes equations are capable to predict the turbulence flow in all its complexity. Unfortunately up to now such accuracy is extremely time-consuming even for relatively simple cases. The barrier is an insufficient computational power. Methods like DNS (Direct Numerical Simulations) which solve the exact Navier-Stokes equations are limited mostly to very simple cases at relatively modest Reynolds numbers. Thus, in order to predict the high turbulent flow behaviour in complex geometries, models based on the original Navier-Stokes equations were developed. The two most popular approaches are LES (Large Eddy Simulation) and RaNS (Reynolds averaged Navier Stokes). In this work the RaNS approach is used. The idea behind RaNS is to split the turbulent quantities in their ensemble averaged value and the turbulent fluctuating component. The ensemble averaged Navier-Stokes equations can be rewritten in terms of the averaged quantities. However unclosed terms contained products of fluctuating values need to be modelled. These terms are namely the Reynolds stress term and the turbulent heat transfer tensor. The "closure" relations make generally use of extra transport equations which involves averaged flow quantities. One of the most common way to model the Reynolds stresses is the assumption that turbulent stresses are proportional to the mean velocity gradient via the turbulent eddy viscosity (eddy viscosity modelling). According to Boussinesq approximation the problem is than shift on the definition of the turbulent eddy viscosity. The eddy viscosity has the dimension of a square length per time unit and is then univocally determined by a typical turbulent velocity and length scale. The velocity scale is often modelled using an extra transport equation for the turbulence kinetic energy defined as follows:

$$k = \frac{1}{2}\overline{u'^2} \tag{6}$$

Where u' represents the turbulent velocity fluctuations. The length scale is calculated as a function of the turbulence kinetic energy dissipation (ε) or the turbulent kinetic frequency (ω). Depending on the eddy viscosity formulation, two-equation family models: k-ε and k-ω are considered.

2.1 k-ε model

k-ε model assumes that the eddy viscosity is related to the turbulence kinetic energy and turbulence dissipation rate according to relation:

$$\mu_t = C_\mu \rho \frac{k^2}{\varepsilon} \tag{7}$$

Values of the turbulence kinetic energy and turbulence dissipation rate are obtained directly from the differential transport equations of both factors.

$$\frac{\partial(\rho k)}{\partial t} + \nabla \cdot (\rho U k) = \nabla \cdot [(\mu + \frac{\mu_t}{\sigma_k})\nabla k] + P_k - \rho\varepsilon \tag{8}$$

$$\frac{\partial(\rho \varepsilon)}{\partial t} + \nabla \cdot (\rho U \varepsilon) = \nabla \cdot [(\mu + \frac{\mu_t}{\sigma_\varepsilon})\nabla \varepsilon] + \frac{\varepsilon}{k}(C_{\varepsilon 1} P_k - C_{\varepsilon 2}\rho\varepsilon) \tag{9}$$

The robustness and high accuracy, as well as low computational costs make the model an important tool, especially in the industrial applications. The drawback of the model is a poor prediction of the flow behavior in case of non-equilibrium boundary layers. The reattachment point during separation flow calculations is usually under-predicted. Errors occur in the magnitude of the local heat transfer and as a consequence the overall device performances are solved not correctly.

2.2 k-ω model

The k-ω model was developed in order to improve the predictions in the near wall region and reduce the errors in adverse pressure gradient calculations. In order to define the turbulent eddy viscosity, the k-ω model uses a frequency scale (ω) called also specific turbulent dissipation rate.

$$\mu_t = \rho \frac{k}{\omega} \tag{10}$$

Both turbulent kinetic energy and specific dissipation rate are obtained from the solution of the following transport equations developed by Wilcox:

$$\frac{\partial(\rho k)}{\partial t} + \nabla \bullet (\rho U k) = \nabla \bullet [(\mu + \frac{\mu_t}{\sigma_k})\nabla k] + P_k - \beta' \rho k \omega \tag{11}$$

$$\frac{\partial(\rho \omega)}{\partial t} + \nabla \bullet (\rho U \omega) = \nabla \bullet [(\mu + \frac{\mu_t}{\sigma_\omega})\nabla \omega] + \alpha \frac{\omega}{k} P_k - \beta \rho \omega^2 \tag{12}$$

The major advantage of the k-ω model is the robust and simple way how the near wall region is handled. Contrary to the k-ε model, the k-ω model does not involve complex non-linear damping functions to take into account the near wall low-Reynolds effects. Due to the non-linearities of the low-Re dumping functions, the k-ε models typically require a higher near wall resolution than the k-ω model (i.e. for the k-ε low-Re models a near wall resolution of $y+ < 0.2$ is often required whereas for the k-ω model a less strict condition of $y+ < 2$ is sufficient) (Vieser, Esch, & Menter, 2002). In complicated industrial applications it is often impossible to resolve with such a grid resolution the boundary layer, therefore the wall function approach is still very popular. In order to improve the accuracy of industrial calculations the k-ω model implemented in the CFX code has the ability to smoothly shift between low-Re number formulation and a wall function scheme depending on the wall y+ resolution. The main weakness of the k-ω model is the strong sensitivity of the solution to the free stream ω values.

2.3 SST model

In order to gather the best from the k-ε and the k-ω models, a new blended model called SST (Shear Stress Transport) model has been available in CFX. The SST model calculates the flow in the near wall region using a k-ω formulation whereas in the bulk flow the high Reynolds k-ε formulation is employed. A smooth transition between the two formulations is ensured by the use of additional blending factors which are functions of the wall distance. To avoid excessive shear stress value in adverse pressure gradient conditions, the turbulent shear stress in the boundary layer is limited based on the Bradshaw assumption of direct proportionality with the kinetic energy ($\tau = \rho a_1 k$).

$$\mu_t = \rho \frac{a_1 k}{\max(a_1 \omega; SF_2)} \tag{13}$$

As in the k-ω model, the CFX implementation of the SST model permits the automatically shifting from the low-Re number formulation to the wall function scheme according to the grid resolution.

3 Numerical model

The geometry of the two-dimensional sudden expansion channel and the location of the coordinate system are depicted in *(Figure 1).* Air enters the computational domain upstream of the step. Across the bottom wall, downstream of the step, a constant heat flux is prescribed. The top wall was considered adiabatic and no-slip velocity boundary conditions were employed. The geometry parameters based on the step high H are the following: the length of the domain is 40 H, the height upstream of the step is equal to 4 H and downstream 5 H for an expansion ratio of 1.25. The Reynolds number based on the step high during the steady-state calculation was fixed to 28 000 and for transient computations with pulsating velocity it varies in the range from 23 000 to 33 000.

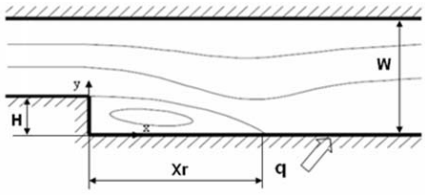

Figure 1: *Geometry and flow configuration for the backward-facing step calculations.*

The computational domain consists of 230 000 unstructured elements. Most of them are placed in the region close to the step and heated wall. The resolution of the grid has a significant effect on the numerical results, thus several trial meshes with different element density and distribution were investigated.

4 Stationary flow

Numerical steady-state results with different turbulence models present a good agreement with the experimental data *(Figure* 2*).* All models predicted the same general behaviour of the flow over the backward facing step. The skin friction coefficient is assumed negative in the recirculation zone and positive downstream. The reattachment point is defined as the axial position where the skin friction coefficient changes from negative to positive values. Downstream of the reattachment point, a recovery zone with monotonically increasing skin friction coefficient is observed. The presence of a secondary recirculation bubble, close to the step corner is also visible. The reattachment length based on the step high obtained by the experiments was approximately equal to 6.67 H (Vogel & Eaton, 1985). Both the k-ω and SST turbulence models predicted the reattachment length with an error less than 3% and respectively 6.74 H and 6.82 H. The position of the maximal negative skin friction coefficient was also predicted correctly, as well as its magnitude. More significant errors are observed for the k-ε model. The reattachment point is predicted about one step height closer to the step, at a position of 5.66 H. The secondary recirculation bubble which appears close to the step corner is hardly visible despite the grid resolution. The overall error it is of the order of 15% and consistent with other numerical investigations (Valencia, 1997). All models presented significantly underestimate the skin friction coefficient in the recovery zone.

The behaviour of the Stanton number is generally opposite to the skin friction coefficient. The investigated models predicted the same, typical behaviour. A sudden drop of the heat transfer coefficient just downstream of the step is followed by a sharp increase till its maximum value near

the reattachment point and by monotonic decrease further downstream in the recovery region. Both, k-ω and SST models predicted almost exactly the position of the maximal Stanton number peak. The SST model also predicted correctly the peak magnitude, whereas the other models gave a significant underestimation. The k-ε model Stanton number values seem to be shifted, similar to the skin friction coefficient results, upstream *(Figure 2).*

In steady flow conditions, the maximal heat transfer can be correlated to the skin friction coefficient and the level of turbulence intensity. The flow in the backward facing step just behind the step is almost stagnant and laminar. Downstream of the step, near the heated wall, the flow turbulence suddenly increases to its maximal value up to the point of maximal heat transfer coefficient. In the recovery region, the turbulence level decreases slowly. Similar behaviour is observed in the Stanton number. The difference in the location between the maximal peaks in the Stanton number and turbulence level is around 0.7 of the step height. This suggests that the Stanton number is considerably controlled by the turbulence level. It could be noticed that the Reynolds analogy does not hold in the recirculation region, in which poor agreement between the Stanton number and skin friction coefficient exists. Downstream in the recovery region, the skin friction coefficient and the Stanton number behave as in the turbulent flat plate solution and the validity of the Reynolds analogy is recovered.

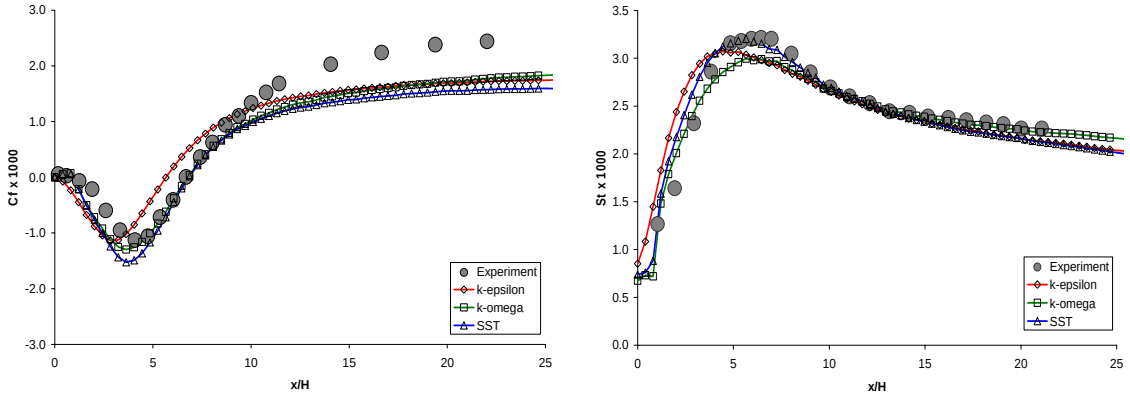

Figure 2 : *Comparison of the skin friction coefficient (left) and Stanton number (right) for the k-ε, k-ω and SST turbulence model.*

4.2 Transient flow

Transient calculations were performed using pulsating inlet velocity. The turbulence model used was the SST model which gave the best prediction in the steady-state configuration. In order to investigate the influence of the pulsating flow on the recirculation region and the heat transfer coefficient, several calculations were performed at different forcing frequency: 10, 100, 400 and 1000 Hz. The corresponding Strouhal number ranges from 0.035 for the 10 Hz excitation to 3.5 for the excitation equal to 1000 Hz. The oscillation amplitude was fixed to 0.2. The Reynolds number based on the step height is varied in the range of 22 000 - 33 000. The calculations time step has been adjusted depending on the frequencies and 10 or 20 samples per cycle were output. The mean values of the skin friction coefficient and Stanton number are obtained by averaging instantaneous values over one cycle. Other geometrical and boundary parameters, as well as grid resolution were undisturbed. Unfortunately no experimental data are available for the unsteady case and the steady-state experimental data are plotted just for comparison.

The pulsations of the inlet velocity caused a variation in the reattachment length. In all investigated cases the primary recirculation bubble grows up together with the decreasing of the inlet velocity. A similar behaviour has been found also for the secondary bubble placed near the step corner. As already shown the length of the recirculation region significantly affects the skin friction coefficient

and Stanton number. Thus both profiles oscillate according to the recirculation bubble configuration *(Figure* 3*)*. In all cases the instantaneous maximal negative peak was several times higher than in the steady-state calculations. Also its axial position varied together with the changes in the recirculation zone. The instantaneous changes in the magnitude and location of the maximal skin friction coefficient did not affect significantly its mean value. For the Strouhal numbers investigated in the range 0.35 - 3.5, the mean maximal peak in the skin friction coefficient has almost the same magnitude and position as the one in the steady-state calculations. The main average trend is as well in good agreement with the steady-state results *(Figure* 3*)*.

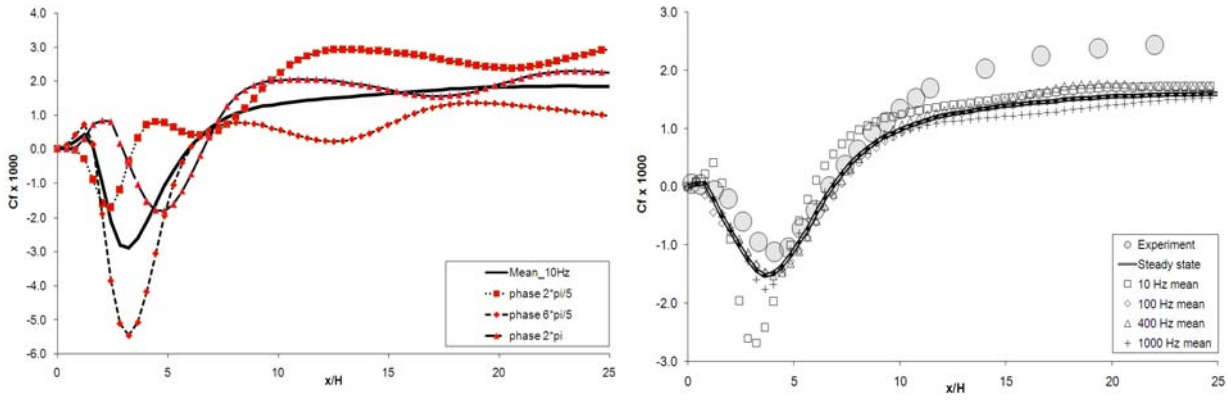

Figure 3: *Skin friction coefficient: transient (10 Hz case - left) and mean (right) results*

In the 10 Hz frequency case, the mean profile differs significantly from the steady-state results. The mean value of the maximal negative peak in the skin friction coefficient is two times higher and shifted upstream of the domain in comparison to the steady-state profile. Thus the mean recirculation region is also shorter. The secondary bubble formed near the step corner with positive axial velocity is clearly visible. In the recovery region, the mean skin friction coefficient profile presents similar behaviour as in the steady-state case. This behaviour of the mean skin friction coefficient profile can be explained as a result of significant changes in the instantaneous velocity profiles. The secondary bubble formed near the step has a major influence on the skin friction coefficient. During the excitation the secondary bubble grows up together with the decreasing of the inlet velocity till its maximal length. At this point, the velocity starts to decrease. As a result of the time delay between changes in the velocity profile and response of the recirculation region and the secondary bubble, the recirculation zone is broken up in two separate parts. Thereafter, the part close to the step behaves like the main recirculation region. Inside this region the secondary bubble is formed again. The part far of the step disappears with the time advancing and a whole cycle is repeated again. During the 10 Hz excitation cycle, it has not been possible to specify exactly the instantaneous reattachment point because of the simultaneous presence of two separate recirculation bubbles in the near wall region. A similar behaviour was observed in low frequency structures in a DNS of the flow over the backward facing step without heat transfer by Le, Moin and Kim (Le, Moin, and Kim, 1997).

For 10 Hz excitation, the transient changes in the heat transfer coefficient are significant. The maximal peak in Stanton number corresponds exactly at the maximum peak of the skin friction coefficient. Due to the recirculation bubble broken up phenomena above described, the maximal peaks in skin friction and heat transfer are moving up and down, backward and forward, depending on the recirculation zone position *(Figure* 4*)*. As a consequence, the mean Stanton number profile for 10 Hz excitation frequency is significantly changed. The maximal peak in Stanton number is higher and shifted upstream. The mean temperature field near the wall is however little affected by the fast, transient changes in the velocity field. Hence, the mean values of the Stanton number profiles agree well with steady-state numerical results especially for high frequency *(Figure* 4*)*.

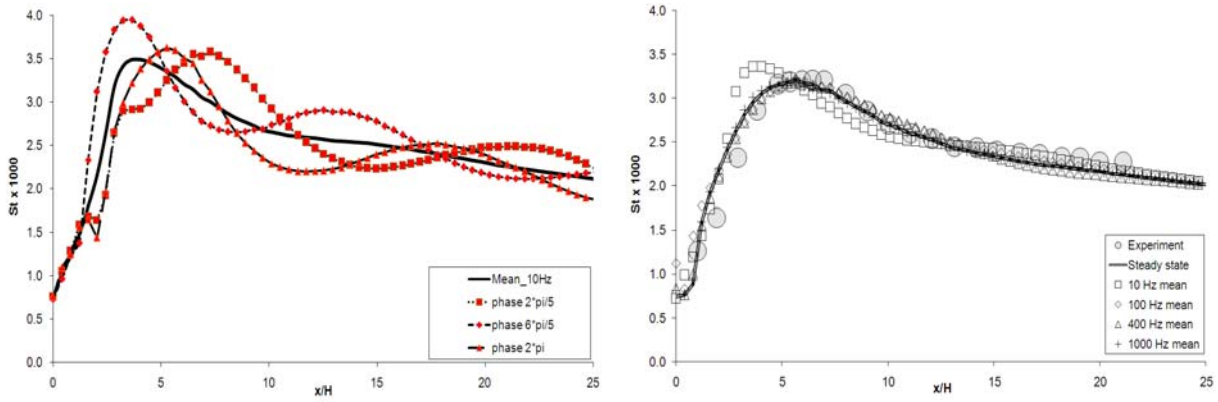

Figure 4: *Stanton number: transient (10Hz case - left) and mean (right) results*

5 Conclusions

For steady inlet flow conditions, all the turbulence models investigated showed good agreement with the experimental data on the skin friction coefficient and the Stanton number. The k-ε model, however, revealed a 15% under-prediction of the reattachment length. The k-ω and SST turbulence models presented an error smaller than 3%.

The effect of the pulsating inlet velocity is especially significant at the excitation frequency of 10 Hz. In this case the secondary recirculation bubble formed in the corner of the step is broken up in two parts. In all cases the instantaneous maximal negative velocity peak was several times bigger than in the steady-state calculations.

Its instantaneous position varied together with the changes in the recirculation zone length. The variations in the wall position affected the transient values of both the skin friction coefficient and the Stanton number, but the time mean values were left almost unchanged. Only in the case of the 10 Hz excitation frequency minor changes were observed.

Acknowledgment

This work is performed in the EU sponsored project FLUISTCOM in the Marie Curie Program, contract number MRTN-CT-2003-504183. The authors would like to thank CFX-ANSYS for the use of the code.

References

Anonymous, CFX 10. (2005). *Online Documentation*.

Le, H., Moin, P., & Kim, J. (1997). Direct numerical simulation of trubulent flow over a backward-facing step. *J. Fluid Mech. , 330*, 349-374.

Valencia, A. (1997). Effect of pulsating inlet on the turbulent flow and heat transfer past a backward-facing step. *Int. Comm. Heat Mass Transfer , 24*, 1009-1018.

Vieser, W., Esch, T., & Menter, F. (2002). *Heat Transfer Predictions using Advanced Two-Equation Trubulence Models.* CFX Validation Report.

Vogel, J., & Eaton, J. (1985). Combined Heat Transfer and Fluid Dynamics Measurements Downstream of a Backward-Facing Step. *Journal of Heat Transfer , 107*, 1009-1018.